RSC Advances

PAPER

View Article Online
View Journal | View Issue

Check for updates

Cite this: *RSC Adv.*, 2019, **9**, 27224

Activating peroxymonosulfate by halogenated and methylated quinones: performance and mechanism†

Hong Zhang,‡[ab] Lina Qiao,‡[b] Jing He,[ab] Na Li,[ab] Dongmei Zhang,[ab] Kai Yu,[ab] Hong You[ab] and Jie Jiang *[ab]

Activation of peroxymonosulfate (PMS) by halogenated and methylated quinones for destroying sulfamethoxazole (SMX) was investigated, where 2,6-dimethyl-1,4-benzoquinone (DMBQ), 2,6-dichloro-1,4-benzoquinone (DCBQ), and tetrafluoro-1,4-benzoquinone (TFBQ) were chosen as model quinones. The PMS could be activated by halogenated and methylated quinones efficiently for SMX degradation, and the process showed high pH and quinones dependency. Different from PMS activated by ultraviolet (UV), singlet oxygen ($^1O_2$) instead of hydroxyl radical ($^{\bullet}OH$) and sulfate radical ($SO_4^{\bullet-}$) was the primary oxidizing species in the activation process. The formation of $^1O_2$ was confirmed by various quenching studies combined with chemical probes (9,10-diphenylanthracene (DPA)). By sampling *in situ* and monitoring in real time, droplet spray ionization mass spectrometry (DSI-MS) was applied to capture and identify the intermediates generated in the activation process. A possible mechanism for PMS activation was proposed accordingly. It was found that a series of reactions between PMS and halogenated/methylated quinones formed a dioxirane intermediate, and the subsequent decomposition of this intermediate produced the $^1O_2$. These findings would help to better understand the interactions between PMS and quinones, and provide a novel activator for PMS activation toward environmental contaminants.

Received 25th June 2019
Accepted 23rd August 2019

DOI: 10.1039/c9ra04789a

rsc.li/rsc-advances

Open Access Article. Published on 30 August 2019. Downloaded on 8/16/2024 4:20:25 PM.
This article is licensed under a Creative Commons Attribution-NonCommercial 3.0 Unported Licence.

1. Introduction

Advanced oxidation processes (AOPs) for the remediation of contaminated soils, groundwater, and sediments have received considerable attention in recent years.[1–3] These processes are based mostly on activation of hydrogen peroxide (H_2O_2),[4] titanium dioxide (TiO_2),[5] persulfate (PDS)[6,7] and peroxymonosulfate (PMS)[8–10] to generate oxidizing species such as sulfate radical ($SO_4^{\bullet-}$) (2.5–3.1 V) and hydroxyl radicals ($^{\bullet}OH$) (1.9–2.7 V),[11] which are highly reactive oxidants toward organic compounds. Among AOPs, PMS has emerged as a popular technique in environmental remediation. Because PMS has high potential of 1.82 V (ref. 12) in generating $SO_4^{\bullet-}$ and $^{\bullet}OH$,[13,14] it has been regarded as an alternative of other methods such as H_2O_2. The application of PMS in destroying refractory organics has been extensively investigated and well-documented.[12,15,16]

To date, various strategies have been developed for activating PMS.[12,16] Generally, the activators for PMS activation include homogenous and heterogeneous transition metal catalyst, metal-free heterogeneous catalysts, ultraviolet, ultrasound, conduction electron, and miscellaneous activation. These techniques can efficiently destroy organic pollutants, but they have significant limitations in the application. As an example, ultrasound, UV, and heating are an environmentally friendly and applicable technology. However, they are not cost-effective for water treatment because of the high-energy consumption. Many studies regarding to PMS activation have focused on transition metals, among which Co(II) is found to be very active in initiating sulfate radical generation from PMS.[17] But the adverse effect of Co(II) on human health needs to be considered. Meanwhile, concerns about metal leaching result in secondary contamination to water body.[18] Therefore, the development of green methods for PMS activation is an area of active research and highly desired.

Quinones such as 1,4-benzoquinone (p-BQ) can efficiently activate PMS with singlet oxygen ($^1O_2$) evolution.[11] It is notable that quinones are potent redox active compounds and ubiquitous in soils, surface water and even in atmospheric aerosols.[19,20] Halogenated quinones can active H_2O_2 to produce $^{\bullet}OH$ by generating a nucleophilic adduct intermediate, but methylated quinones fail to active H_2O_2.[21] Furthermore, halogenated

[a]School of Marine Science and Technology, Harbin Institute of Technology at Weihai, Weihai, Shandong 264209, P. R. China. E-mail: jiejiang@hitwh.edu.cn; Fax: +86-631-5685-359

[b]State Key Laboratory of Urban Water Resource and Environment, Harbin Institute of Technology, Harbin, Heilongjiang 150090, P. R. China

† Electronic supplementary information (ESI) available. See DOI: 10.1039/c9ra04789a

‡ These authors contributed equally to this work.

This journal is © The Royal Society of Chemistry 2019

Open Access Article. Published on 30 August 2019. Downloaded on 8/16/2024 4:20:25 PM.
This article is licensed under a Creative Commons Attribution-NonCommercial 3.0 Unported Licence.

and methylated quinones are also effective in activating PDS with $SO_4^{\bullet -}$ evolution by a semiquinone radical-dependent mechanism.[20] However, little is known about the halogenated and methylated quinones on PMS activation so far.

The goals of the present work are (i) to investigate the activation of PMS by halogenated and methylated quinones to catalytically oxidize organic pollutants, (ii) to capture and identify the primary oxidizing species during the activation process, and (iii) to elucidate the mechanism of PMS activated by halogenated and methylated quinones. Herein, activations of PMS by halogenated and methylated quinones for sulfamethoxazole (SMX) removal under various conditions were examined. SMX was chosen as target contaminant, since SMX is very stable and has been frequently detected in soils and water sources. Chemical trapping methods combined with various radical scavengers have been employed to investigate the oxidizing species in the activation process. *In situ* characterization using droplet spray ionization mass spectrometry (DSI-MS) was applied to analyze the intermediates generated in the catalytic PMS decomposition process. Results indicated that the combination of PMS with halogenated and methylated quinones is an attractive process providing efficient $^1O_2$ generation for SMX degradation.

In a DSI-MS experiment, a corner of cover slip placed in front of the MS inlet functions as the spray corner and solution reservoir. By applying a high voltage to the solution, a charged-droplet spray is formed between the corner and the MS inlet.[22,23] DSI-MS addresses the detection limitation in the sample transfer capillary of electrospray ionization and can monitor chemical reactions in real time. Applications of DSI-MS have included real-time monitoring of photolysis/photocatalysis reactions,[24,25] catalytic reactions,[22,26] and electrochemical reactions[27,28] where the intermediates are fished out and characterized by MS. DSI is particularly suitable for fast reaction kinetics and short-lived reactive intermediates involved reaction.

2. Materials and methods

2.1 Materials

Methanol and acetonitrile at MS grade were purchased from Sigma-Aldrich (Darmstadt, Germany). Benzoic acid (BA), 9,10-diphenylanthracene (DPA), and sodium azide (NaN_3) were purchased from Sigma-Aldrich (St. Louis, MO). Ethanol, sodium borate ($Na_2B_4O_7 \cdot 10H_2O$), and sodium thiosulfate ($Na_2S_2O_3$) were purchased from Aike Co. (Chengdu, Chian). Sulfamethoxazole (SMX), 2,6-dimethyl-1,4-benzoquinone (DMBQ), 2,6-dichloro-1,4-benzoquinone (DCBQ), and tetrafluoro-1,4-benzoquinone (TFBQ) were obtained from J&K Scientific Ltd. (Beijing, China). The structures of the quinones investigated in this study were given in Table S1.† Ultrapure water was obtained from a Milli-Q water purification system. All the individual solutions were freshly prepared before use.

2.2 Experimental procedure and analysis

The removal of SMX by PMS in the presence of DMBQ, DCBQ and TFBQ was conducted in a brown flask on a reciprocating shaker at 25 ± 1 °C in the dark. This aimed to avoid decomposition of quinones and PMS by light irradiation. The experiments were carried out by simultaneously adding different quinones (1–20 μM) and PMS (0.5 mM) into pH-buffered solutions (20 mM sodium borate; pH 7–10) containing SMX (10 μM). All samples were collected at regular time points, quenched with sodium thiosulfate, and stored at 4 °C before being analyzed by LC-MS/MS.

A Thermo Finnigan Surveyor LC coupled to a Thermo LTQ mass spectrometer equipped with an electrospray ionization source was used for LC-MS/MS analysis. An Agilent ZORBAX Eclipse plus C18 column (150 × 4.6 mm, 3.5 μm) was used for analytes separation. The isocratic mobile phase consisted of 70% acetonitrile and 30% water containing 0.1% formic acid, and the flow rate was 1 mL min^{-1}. To avoid contamination of the mass spectrometer, a switching valve was used to divert the LC fluid to the waste bottle during the first and last few minutes. The MS parameters were set as follows: spray voltage, 4.5 kV; capillary voltage, 50 V; tube lens, 110 V; capillary temperature, 275 °C; ion maximum injection time, 20 ms; auxiliary gas, 35 arbitrary units; sheath gas, 4 arbitrary units; ion pair for SMX, 254/156. Each experiment was conducted in triplicate, and the averaged data and standard deviation were presented.

2.3 Chemical detection of singlet oxygen

DPA was used to trap the $^1O_2$ formed in PMS activated by different quinones (DMBQ, TCBQ, and TFBQ). The corresponding DPA endoperoxide ($DPAO_2$) can be detected by MS.[29] Experiments were conducted in a mixed solution of 0.5 mM PMS, 20 μM different quinones (DMBQ, TCBQ, and TFBQ), and 20 μM DPA in 20 mM sodium borate buffer at pH 10. The reaction was allowed to react for 60 min. After dilution and filtration, the solution was analyzed by LC-MS/MS operated in the positive ion mode.

2.4 Intermediate identification

To identify the intermediates in PMS activated by DMBQ, DCBQ and TFBQ, *in situ* analysis and real-time monitoring of the reaction of PMS and quinones were carried out by droplet spray ionization mass spectrometry (DSI-MS). A detailed description of DSI-MS is given elsewhere.[22,24] A photograph of the DSI-MS is shown in Fig. S1.† The protocol for *in situ* analysis and real-time monitoring of PMS activated by different quinones involved three steps (Fig. S2†). Firstly, 10 μL of methanol/water (v/v: 7/3) was loaded onto the corner at 0 s. When a high voltage of −4 kV was applied to the solution, an electrospray was formed between the corner and the MS inlet. Then, 10 μL of different quinones (DMBQ, TCBQ, and TFBQ) (5×10^{-5} mol L^{-1}) was loaded onto the corner at 10 s. Finally, 30 μL of PMS (5×10^{-4} mol L^{-1}) was loaded onto the corner at 14 s. Data were recorded continuously during these additions of reagents. The sample solutions were adjusted at pH 10 before pipetting to the corner. These experiments were implemented on a Thermo LTQ-Orbitrap XL mass spectrometer (Thermo Fisher Scientific, Waltham, MA, USA). The operation parameters were set as follows: resolution, 60 000; capillary temperature, 275 °C; ion

Open Access Article. Published on 30 August 2019. Downloaded on 8/16/2024 4:20:25 PM.
This article is licensed under a Creative Commons Attribution-NonCommercial 3.0 Unported Licence.

maximum injection time, 500 ms; tube lens voltage, −110 V; capillary voltage, −35 V.

3. Results and discussion

3.1 Effect of pH on SMX degradation

The degradations of SMX by PMS in the presence of DMBQ, DCBQ and TFBQ over a pH range of 7–10 were conducted, and the results are shown in Fig. 1. In the absence of quinones, the degradation of SMX by PMS was negligible within the pH investigated. Comparatively, SMX degradation gradually increased from pH 7 to 10 by PMS in the presence of quinones. For instance, when the PMS was in the presence of DMBQ, the degradation of SMX in 9 min increased from 7% to 70% with pH from 7 to 10. In the case of PMS/DCBQ in 9 min, with the increase of pH from 7 to 10, the degradation of SMX increased from 12% to 100%. As for PMS/TFBQ in 9 min, the degradation of SMX at pH 7 was only 16%, while that of SMX at pH 10 reached 100%. In addition, the first-order rate constants derived from Fig. 1 were listed in Table S1.† These rate constants also suggest that pH has a significant effect on the SMX degradation. For instance, in the case of PMS/TFBQ, with increasing pH from 8 to 10, the degradation rate increased from 0.0702 to 0.6323 min^{-1}. Moreover, the pH in experiment of pH 10 showed negligible change (Fig. S3†).

After the reactions, residual contents of PMS over pH 7–10 were also determined (Fig. S4†). In control experiments with PMS alone, the decomposition of PMS was negligible within the pH investigated. However, when the PMS was in the presence of quinones, the degradation of PMS significantly enhanced with the increase of pH from 7 to 10. This pH dependent decomposition of PMS was consistent with SMX degradation (Fig. S4† and 1). Therefore, pH adjustment may be a good option to enhance reaction rates if necessary.

3.2 Effect of quinones concentrations on SMX degradation

The degradations of SMX by PMS under different concentrations of quinones were also investigated. From Fig. 2, the degradation of SMX significantly enhanced with the increase of quinones concentrations. For instance, in the case of PMS/DCBQ in 9 min, SMX degradation increased from 42% to 98% with the DCBQ concentrations from 10 to 20 μM. As for PMS/TFBQ in 6 min, the SMX degradation was only 40% when the concentration of TFBQ was 10 μM; whereas the SMX was completely degraded at the concentration of 20 μM.

As shown in Fig. 2, in control experiments with quinones alone, the SMX degradation was negligible. This observation indicates that the relatively strong oxidant semiquinone radicals appeared in quinones solution[20] could not directly degrade SMX. Similar results have also been reported in previous studies.[11] These results suggest that halogenated and methylated quinones can significantly enhance the degradation of SMX by PMS. From Fig. 1 and 2, it seems that SMX degraded by PMS showed both pH and quinones dependency.

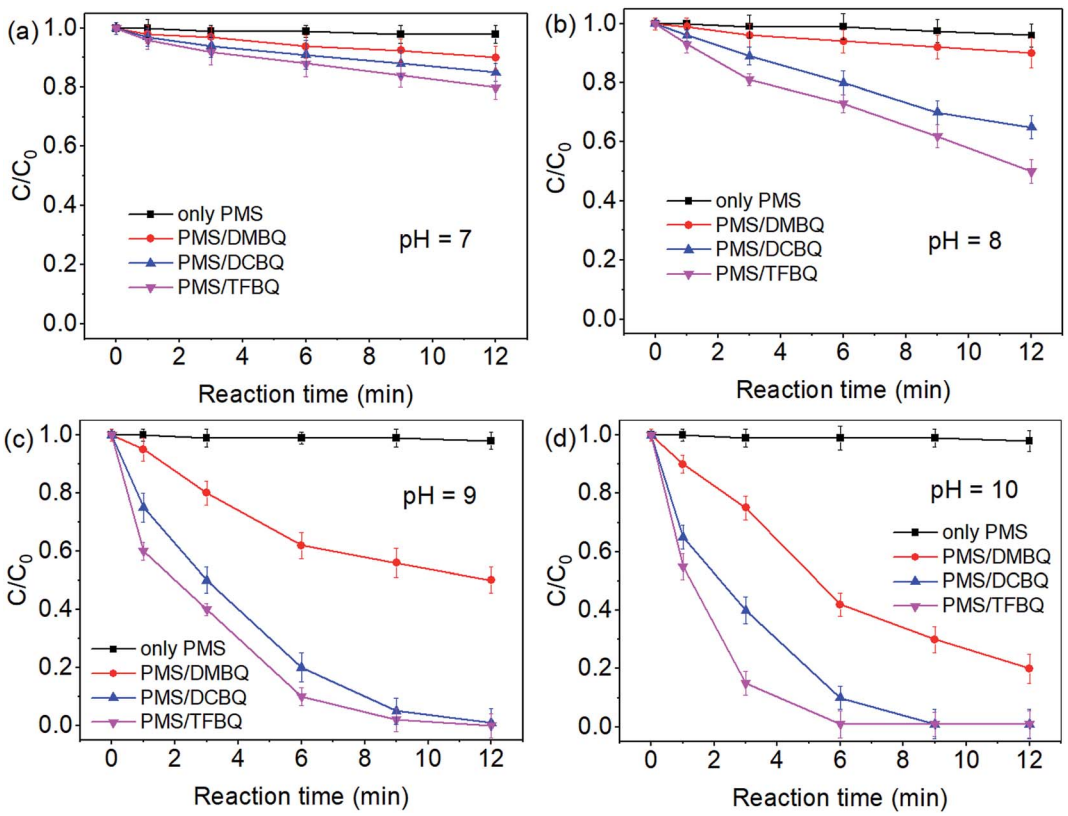

Fig. 1 Effect of pH on SMX degradation. (a) pH 7; (b) pH 8; (c) pH 9; (d) pH 10. Experimental conditions: $[PMS]_0 = 0.50$ mM, $[SMX]_0 = 10$ μM, $[BQ]_0 = 20$ μM, 20 mM borate buffer, and $T = 25$ °C.

This journal is © The Royal Society of Chemistry 2019

Open Access Article. Published on 30 August 2019. Downloaded on 8/16/2024 4:20:25 PM.
This article is licensed under a Creative Commons Attribution-NonCommercial 3.0 Unported Licence.

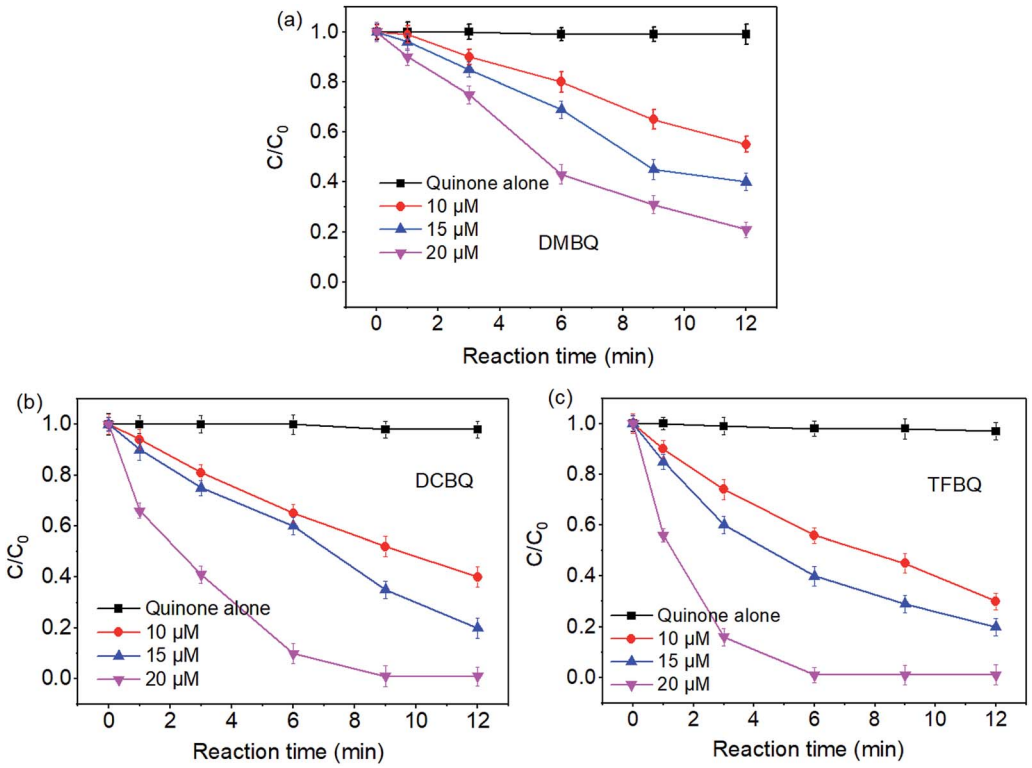

Fig. 2 Effect of quinones concentrations on SMX degradation. (a) DMBQ; (b) DCBQ; (c) TFBQ. Experimental conditions: $[PMS]_0 = 0.50$ mM, $[SMX]_0 = 10$ μM, 20 mM borate buffer, pH = 10, and $T = 25$ °C.

3.3 Identification of oxidizing species

3.3.1 Specific quenchers. Generally, $^{\bullet}OH$ and $SO_4^{\bullet-}$ are the oxidizing species during oxidation involving PMS,[30,31] and $^1O_2$ may also be formed.[11] Because these three-oxidizing species show high reactivity toward SMX, effect of quenchers on SMX degradation was tested to identify the oxidizing species. Methanol and ethanol are widely used quenchers for $^{\bullet}OH$ and $SO_4^{\bullet-}$ (Table S3†),[20] but they are inefficient for $^1O_2$. In contrast, NaN_3 is an efficient quencher for $^1O_2$ with a rate constant of 1.0×10^9 M^{-1} s^{-1}.[32] Therefore, if $^{\bullet}OH$ and $SO_4^{\bullet-}$ are the dominant oxidizing species, methanol and ethanol in excess (0.1 M) would significantly quench the oxidizing species, and thus the degradation of SMX. As shown in Fig. S5,† methanol and ethanol failed to impede the SMX degradation. In addition, BA, a typical probe compound for $^{\bullet}OH$ and $SO_4^{\bullet-}$ was also tested. The result in Fig. S6† showed that the combination of PMS with different quinones (DMBQ, DCBQ, and TFBQ) could not destroy BA efficiently, even when the reaction time was prolonged to 30 min.

Comparatively, the degradation of SMX markedly slowed down when NaN_3 was added, as shown in Fig. 3. For instance, SMX was completely degraded in 20 min without NaN_3; whereas with 0.1 M NaN_3 added, only 20%, 23% and 29% SMX were degraded by PMS in the presence of DMBQ, DCBQ and TFBQ, respectively. These results indicated that neither $^{\bullet}OH$ nor $SO_4^{\bullet-}$ were formed, and that $^1O_2$ may be the primary oxidizing species that lead to the degradation of SMX.

3.3.2 Chemical trapping. To further identify the oxidizing species, DPA was used to chemically trap the $^1O_2$. This method is based on that the rapid and specific reaction of $^1O_2$ with DPA ($k_r = 1.3 \times 10^6$ M^{-1} s^{-1}) forms a stable DPA endoperoxide ($DPAO_2$),[33] which can be detected by mass spectrometer operated in the positive ion mode. The combination of PMS/different quinones with DPA all produced the corresponding $DPAO_2$ at m/z 363 (data not shown). When subjected to MS/MS experiments, the endoperoxide at m/z 363 in each case showed an intense fragment ion at m/z 330 corresponding to radical cation of DPA (Fig. 4a). This result is consistent with previous studies where the endoperoxide reproduced the radical cation of DPA.[26,33] In addition, the intensity of $DPAO_2$ gradually increased with increasing the concentrations of PMS from 100 to 300 μM (Fig. 4b). The signal of $DPAO_2$ was not observed in

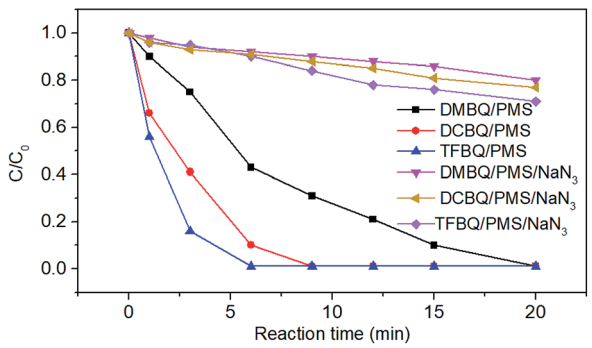

Fig. 3 Effect of scavengers on SMX degradation in PMS activated by DMBQ, DCBQ and TFBQ. Experimental conditions: $[PMS]_0 = 0.50$ mM, $[Quinone]_0 = 20$ μM, $[SMX]_0 = 10$ μM, 20 mM borate buffer, pH = 10, and $T = 25$ °C.

Open Access Article. Published on 30 August 2019. Downloaded on 8/16/2024 4:20:25 PM.
This article is licensed under a Creative Commons Attribution-NonCommercial 3.0 Unported Licence.

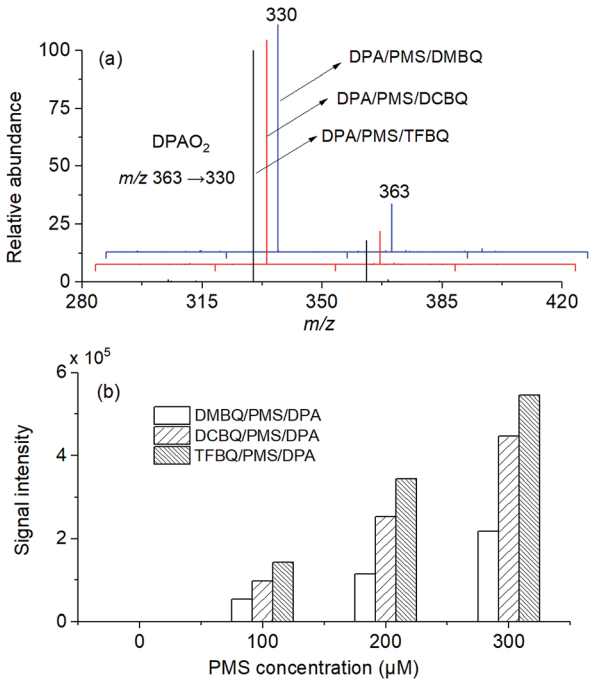

Fig. 4 (a) MS/MS spectra of $DPAO_2$ generated in PMS/different quinones/DPA; (b) effect of PMS concentrations on the generation of $DAPO_2$.

blank experiment without PMS (Fig. 4b). These results suggested the involvement of $^1O_2$ in the reaction of PMS with different quinones (DMBQ, DCBQ, and TFBQ).

3.4 Activation mechanism

3.4.1 Intermediate identification. To elucidate the activation mechanism between PMS and quinones (DMBQ, DCBQ, and TFBQ), identification of the intermediates generated in the activation process was performed. The intermediates were firstly investigated by LC-ESI-MS to collect information that could elucidate the mechanism of PMS activated by quinones (DMBQ, DCBQ, and TFBQ). Because of the complex pretreatments, the LC-ESI-MS technique failed to provide information on the intermediates (data not shown). Droplet spray ionization mass spectrometry (DSI-MS) can offer *in situ* and real-time information for reactions.[22] DSI-MS has been applied to capture and characterize photolysis reaction intermediates,[24,25] dioxirane intermediates,[26] and other short-lived intermediates.[23,34] Therefore, *in situ* analysis and real-time monitoring of PMS activated by quinones (DMBQ, DCBQ, and TFBQ) were performed by DSI-MS. The workflow is shown in Fig. S2.† The real-time mass spectra obtained for the activation reaction are shown in Fig. 5.

In the case of PMS activated by DBMQ (Fig. 5a), the signal at *m*/*z* 136.0522 and 151.0393 corresponded to $DMBQ^{\bullet-}$ and $[DMBQ + O - H]^-$ respectively. Peak at *m*/*z* 137.0600 was assigned as $[DMBQ + H]^-$. This is due to that DMBQ underwent an electrochemical reduction at the spraying tip forming hydro-DMBQ. It is similar to what has been reported in previous studies.[35] The signals at *m*/*z* 112.9542 and 96.9592 were assigned as HSO_5^- and HSO_4^-. In addition, two signals at *m*/*z*

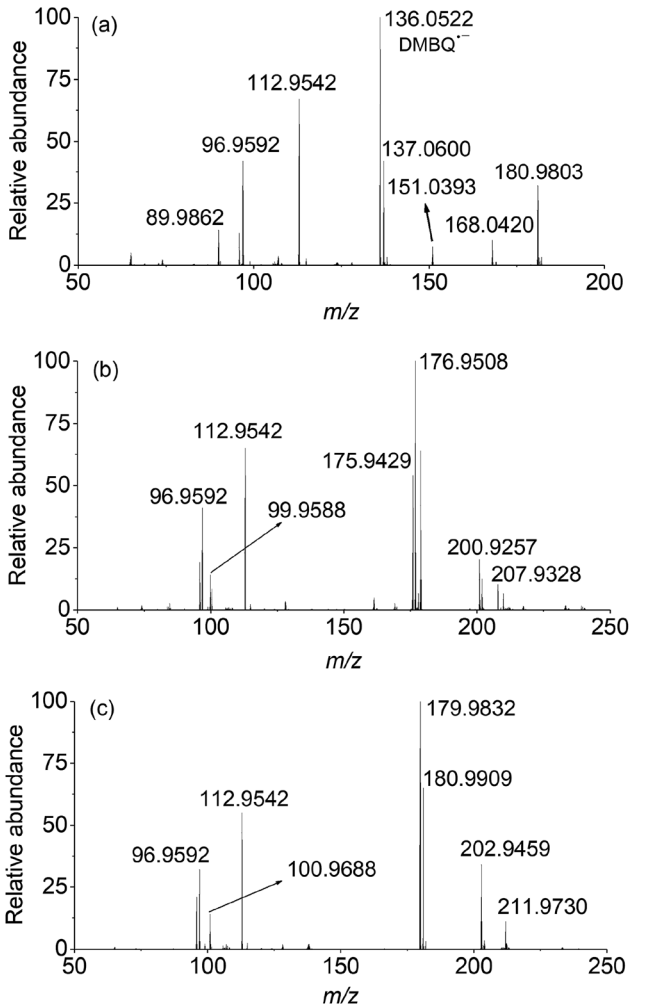

Fig. 5 *In situ* and real-time characterization of intermediates in PMS/different quinones using DSI-MS. (a) PMS/DMBQ, (b) PMS/DCBQ, and (c) PMS/TFBQ. Mass spectra displayed the reaction time of 40 s for each case.

180.9803 and 89.9862 were evident. Peak of *m*/*z* 180.9803 was tentatively assigned as a peroxide adduct intermediate, which is due to nucleophilic addition of two molecules of HSO_5^- to the carbonyl group of DMBQ. Peak of *m*/*z* 89.9862 was attributed to the conjugate base of the adduct intermediate. In this sense, peaks of *m*/*z* 180.9803 and 89.9862 were detected with two and four charges, respectively. The comparison of isotopic envelope and theoretical simulation (Thermo Xcalibur Qual Browser 2.0) clearly confirmed this assumption (Fig. S7 and S8†). To further confirm these assignments, tandem mass spectrometry (MS/MS) was performed for structural characterization. These two ions showed similar dissociation behaviors where both of them gave daughter ions of *m*/*z* 113 corresponding to HSO_5^- (Fig. S9†).

In addition, a signal at *m*/*z* 168.0420, tentatively assigned as a dioxirane intermediate ($[C_8H_8O_4]^{\bullet-}$) was unambiguously observed. The abundance of this ion during mass selection and isolation was absence, even when the isolation window increased from 1 to 10 Th. This suggested that this ion could not be effectively subjected to MS/MS experiments. However, the

 This journal is © The Royal Society of Chemistry 2019

Open Access Article. Published on 30 August 2019. Downloaded on 8/16/2024 4:20:25 PM.
This article is licensed under a Creative Commons Attribution-NonCommercial 3.0 Unported Licence.

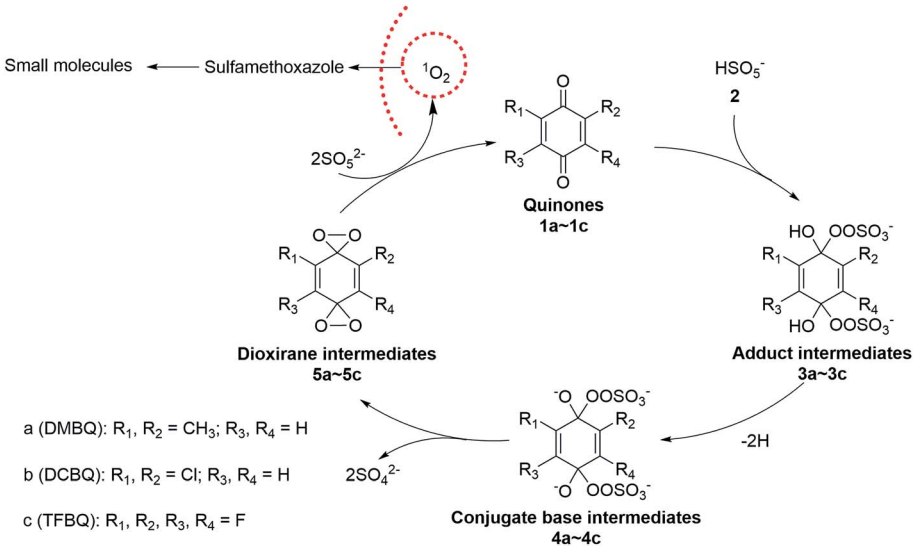

Fig. 6 Possible mechanism of PMS activated by halogenated and methylated quinones.

isotopic envelope of *m*/*z* 168.0420 compared well with theoretical simulation (Fig. S10†). The high accurate mass listed in Table S4† and isotopic envelope of this intermediate sufficiently confirmed the assignment of this ion. Fig. 5b and c depict the mass spectra of PMS activated by DCBQ and TFBQ, respectively. The assignments and high accurate mass of these intermediates/products were listed in Tables S5 and S6.† Furthermore, the dissociation behaviors of these intermediates showed similar characteristic peaks (*m*/*z* 113, HSO_5^-) (Fig. S11 and S12†), which is consistent with PMS activated by DMBQ (Fig. S9†). These results show the same behavior where dissociation of intermediates in activation of PMS by DMBQ, DCBQ and TFBQ generates HSO_5^- and reproduced the corresponding quinones. This also supports the fact that PMS activated by DMBQ, DCBQ and TFBQ followed the same activation pathway.

3.4.2 Possible mechanism of PMS activated by halogenated and methylated quinones. It is well-known that PMS can be catalyzed by ketones in alkaline solutions with $^1O_2$ evolution, where the involvement of a dioxirane intermediate was proposed.[36] In the present work, DMBQ, DCBQ and TFBQ can be considered as a ketone containing two carbonyl groups. Therefore, a possible activation pathway was proposed according to the previous studies and the DSI-MS analysis of intermediates. As shown in Fig. 6, the nucleophilic addition of PMS and quinones firstly forms a peroxide adduct intermediate **3**. Intermediate **3** further converts to intermediate **4**, which is associated with the conjugate base of **3**. By intramolecular nucleophilic displacement reaction of alkoxide oxygen at the O–O bond,[37] intermediate **4** then decomposes to a dioxirane intermediate **5** and releases two molecules of SO_4^{2-}. Finally, intermediate **5** suffers nucleophilic attack by two molecules SO_5^{2-}. This generates the $^1O_2$ and reforms the quinones.

PMS has been activated by various techniques such as heating, UV, p-BQ, and transition metal.[12] In the present study, the activation pathway contrasted with PMS activated by UV and transition metal where $^{\bullet}OH$ and/or $SO_4^{\bullet-}$ are the primary oxidizing species. Because the halogenated quinones have some toxic, we reiterate that this methodology is suitable for the area where halogenated quinones and pollutants simultaneously exist in wastewater and only PMS is added to the system. This avoids the possibility of contaminate from quinones.

4. Conclusion

In conclusion, the activation of peroxymonosulfate (PMS) by halogenated and methylated quinones (DMBQ, DCBQ, and TFBQ) could degrade SMX efficiently in aqueous solution. The kinetic studies suggested that the activation process was pH and quinones dependency, providing a guidance for reaction rate optimization. Chemical trapping combined with special quencher studies revealed that $^1O_2$ instead of $^{\bullet}OH$ and $SO_4^{\bullet-}$ was the primary oxidizing species. This nonradical oxidant was effective in organic oxidation, meanwhile presenting a better selectivity to target contaminants from background organic matters. By sampling *in situ* analysis and monitoring in real time, DSI-MS successfully capture and identify the intermediates/products in the reaction of PMS with different quinones. A mechanism was proposed involving the formation of a peroxide adduct intermediate, a dioxirane intermediate, and the subsequent generation of $^1O_2$. The success in PMS activated by different quinones advances quinone-mediated PMS activation. The differences in behavior associated with the quinone functional groups help the options of the activating reagent. The findings of this study provide a new pathway of PMS activation and efficient degradation technique for environmental contaminants.

Conflicts of interest

The authors declare no competing financial interest.

Acknowledgements

This work was supported by the National Key R&D Program of China (No. 2016YFF0100302), Natural Science Foundation of

Open Access Article. Published on 30 August 2019. Downloaded on 8/16/2024 4:20:25 PM.
This article is licensed under a Creative Commons Attribution-NonCommercial 3.0 Unported Licence.

China (No. 21705030, 21904029) and the Fundamental Research Funds for the Central Universities (No. HIT.NSRIF.2020087).

References

1 X. G. Duan, H. Q. Sun, Z. P. Shao and S. B. Wang, *Appl. Catal., B*, 2018, **224**, 973–982.
2 Z. P. Xing, J. Q. Zhang, J. Y. Cui, J. W. Yin, T. Y. Zhao, J. Y. Kuang, Z. Y. Xiu, N. Wan and W. Zhou, *Appl. Catal., B*, 2018, **225**, 452–467.
3 L. W. Matzek and K. E. Carter, *Chemosphere*, 2016, **151**, 178–188.
4 F. X. Chen, S. L. Xie, X. L. Huang and X. H. Qiu, *J. Hazard. Mater.*, 2017, **322**, 152–162.
5 P. Chen, F. L. Wang, Z. F. Chen, Q. X. Zhang, Y. H. Su, L. Z. Shen, K. Yao, Y. Liu, Z. W. Cai, W. Y. Lv and G. G. Liu, *Appl. Catal., B*, 2017, **204**, 250–259.
6 R. C. Zhang, P. Z. Sun, T. H. Boyer, L. Zhao and C. H. Huang, *Environ. Sci. Technol.*, 2015, **49**, 3056–3066.
7 X. X. Pan, L. Q. Yan, R. J. Qu and Z. Y. Wang, *Chemosphere*, 2018, **196**, 95–104.
8 W. Tang, Y. Zhang, H. Guo and Y. Liu, *RSC Adv.*, 2019, **9**, 14060–14071.
9 J. Zhu, Z. Zhu, H. Zhang, H. Lu and Y. Qiu, *RSC Adv.*, 2019, **9**, 2284–2291.
10 N. Jaafarzadeh, F. Ghanbari and M. Ahmadi, *Chemosphere*, 2017, **169**, 568–576.
11 Y. Zhou, J. Jiang, Y. Gao, J. Ma, S. Y. Pang, J. Li, X. T. Lu and L. P. Yuan, *Environ. Sci. Technol.*, 2015, **49**, 12941–12950.
12 F. Ghanbari and M. Moradi, *Chem. Eng. J.*, 2017, **310**, 41–62.
13 J. Hou, L. Xu, Y. Han, Y. Tang, H. Wan, Z. Xu and S. Zheng, *RSC Adv.*, 2019, **9**, 974–983.
14 X. Zhang, J. Yao, W. Peng, W. Xu, Z. Li, C. Zhou and Z. Fang, *RSC Adv.*, 2018, **8**, 33681–33687.
15 W. Oh, Z. Dong and T. Lim, *Appl. Catal., B*, 2016, **194**, 169–201.
16 P. Hu and M. Long, *Appl. Catal., B*, 2016, **181**, 103–117.
17 G. P. Anipsitakis and D. D. Dionysiou, *Environ. Sci. Technol.*, 2003, **37**, 4790–4797.
18 Y. X. Wang, Z. M. Ao, H. Q. Sun, X. G. Duan and S. B. Wang, *Appl. Catal., B*, 2016, **198**, 295–302.
19 M. Fujii, A. Imaoka, C. Yoshimura and T. D. Waite, *Environ. Sci. Technol.*, 2014, **48**, 4414–4424.
20 G. D. Fang, J. Gao, D. D. Dionysiou, C. Liu and D. M. Zhou, *Environ. Sci. Technol.*, 2013, **47**, 4605–4611.
21 B. Z. Zhu, H. T. Zhao, B. Kalyanaraman and B. Frei, *Free Radical Biol. Med.*, 2002, **32**, 465–473.
22 J. Jiang, H. Zhang, M. Li, M. T. Dulay, A. J. Ingram, N. Li, H. You and R. N. Zare, *Anal. Chem.*, 2015, **87**, 8057–8062.
23 H. Zhang, N. Li, X. D. Li, J. Jiang, D. D. Zhao and H. You, *Rapid Commun. Mass Spectrom.*, 2016, **30**, 51–55.
24 H. Zhang, N. Li, Y. Wang, D. Zhao, J. He, H. You and J. Jiang, *Chemosphere*, 2017, **184**, 932–938.
25 H. Zhang, N. Li, D. Zhao, J. Jiang and H. You, *J. Am. Soc. Mass Spectrom.*, 2017, **28**, 1939–1946.
26 H. Zhang, K. Yu, J. He, N. Li, H. You and J. Jiang, *Microchem. J.*, 2018, **139**, 437–442.
27 K. Yu, H. Zhang, J. He, R. N. Zare, Y. Wang, L. Li, N. Li, D. Zhang and J. Jiang, *Anal. Chem.*, 2018, **90**, 7154–7157.
28 K. Y. Hong Zhang, H. Jing, N. Li, H. You and J. Jiang, *Analyst*, 2018, **143**, 4247–4250.
29 S. Miyamoto, G. R. Martinez, A. P. B. Martins, M. H. G. Medeiros and P. Di Mascio, *J. Am. Chem. Soc.*, 2003, **125**, 4510–4517.
30 W. D. Oh, Z. L. Dong, G. Ronn and T. T. Lim, *J. Hazard. Mater.*, 2017, **325**, 71–81.
31 Y. H. Guan, J. Ma, X. C. Li, J. Y. Fang and L. W. Chen, *Environ. Sci. Technol.*, 2011, **45**, 9308–9314.
32 H. E. Gsponer, C. M. Previtali and N. A. Garcia, *Toxicol. Environ. Chem.*, 1987, **16**, 23–37.
33 S. Miyamoto, G. R. Martinez, M. H. G. Medeiros and P. Di Mascio, *J. Am. Chem. Soc.*, 2003, **125**, 6172–6179.
34 J. Jiang, D. Zhao, H. Zhang, J. He and N. Li, *Anal. Methods*, 2017, **9**, 4201–4206.
35 F. Qin, Y. Y. Zhao, Y. L. Zhao, J. M. Boyd, W. J. Zhou and X. F. Li, *Angew. Chem., Int. Ed.*, 2010, **49**, 790–792.
36 A. R. Gallopo and J. O. Edwards, *J. Org. Chem.*, 1981, **46**, 1684–1688.
37 J. O. Edwards, R. H. Pater and R. Curci, *Photochem. Photobiol.*, 1979, **30**, 63–70.

 This journal is © The Royal Society of Chemistry 2019